The Plant Cell, Vol. 18, 1438–1453, June 2006, www.plantcell.org © 2006 American Society of Plant Biologists

Petunia Phospholipase C1 Is Involved in Pollen Tube Growth [W]

Peter E. Dowd,[a] Sylvie Coursol,[b,1] Andrea L. Skirpan,[a,2] Teh-hui Kao,[a] and Simon Gilroy[b,3]

[a] Department of Biochemistry and Molecular Biology, Pennsylvania State University, University Park, Pennsylvania 16802
[b] Department of Biology, Pennsylvania State University, University Park, Pennsylvania 16802

Although pollen tube growth is essential for plant fertilization and reproductive success, the regulators of the actin-related growth machinery and the cytosolic Ca^{2+} gradient thought to determine how these cells elongate remain poorly defined. Phospholipases, their substrates, and their phospholipid turnover products have been proposed as such regulators; however, the relevant phospholipase(s) have not been characterized. Therefore, we cloned cDNA for a pollen-expressed phosphatidylinositol 4,5-bisphosphate ($PtdInsP_2$)–cleaving phospholipase C (PLC) from *Petunia inflata*, named Pet PLC1. Expressing a catalytically inactive form of Pet PLC1 in pollen tubes caused expansion of the apical Ca^{2+} gradient, disruption of the organization of the actin cytoskeleton, and delocalization of growth at the tube tip. These phenotypes were suppressed by depolymerizing actin with low concentrations of latrunculin B, suggesting that a critical site of action of Pet PLC1 is in regulating actin structure at the growing tip. A green fluorescent protein (GFP) fusion to Pet PLC1 caused enrichment in regions of the apical plasma membrane not undergoing rapid expansion, whereas a GFP fusion to the $PtdInsP_2$ binding domain of mammalian PLC δ1 caused enrichment in apical regions depleted in PLC. Thus, Pet PLC1 appears to be involved in the machinery that restricts growth to the very apex of the elongating pollen tube, likely through its regulatory action on $PtdInsP_2$ distribution within the cell.

INTRODUCTION

After germination on a receptive stigmatic surface, a pollen grain produces a tip-growing pollen tube that must navigate the style, locate the ovary, and deliver the sperm for fertilization. Thus, pollen tube elongation represents highly regulated tip growth required for plant fertility. Tube growth is known to be driven by exocytosis localized to the growing apex, and one element thought to direct this secretory activity is a tip-focused gradient in cytosolic Ca^{2+} (Holdaway-Clarke and Hepler, 2003). Other regulators of pollen tube tip growth include monomeric G-proteins, their interacting proteins (Fu and Yang, 2001; Wu et al., 2001; Chen et al., 2003; Cheung et al., 2003; Gu et al., 2005), and the cytoskeleton (Hepler et al., 2001). However, how these, or other, regulatory elements are integrated with the tip-focused Ca^{2+} gradient to control growth remains poorly understood.

Turnover of membrane lipids modulates a wide range of cellular signaling elements, including the dynamics of the actin cytoskeleton and Ca^{2+} second messenger systems, both important components of the tip growth machinery. For example, the phospholipase Cs (PLCs) can cleave the phospholipid phosphatidylinositol 4,5-bisphosphate ($PtdInsP_2$) to produce two cellular regulators, diacyl glycerol and the Ca^{2+}-mobilizing messenger inositol 1,4,5-trisphosphate ($InsP_3$). PLC has been implicated in processes as diverse as signal transduction in guard cells (Hunt et al., 2003; Mills et al., 2004) and pathogen response (de Jong et al., 2004). $InsP_3$ and other inositol lipid-related compounds have also been proposed as important regulators of pollen tube growth (Franklin-Tong et al., 1996; Malhó, 1998; Zonia et al., 2002; Zonia and Munnik, 2004; Monteiro et al., 2005). Moreover, $InsP_3$ has been shown to release Ca^{2+} from internal stores in plant cells (Alexandre et al., 1990), including pollen tubes (Franklin-Tong et al., 1996; Malhó, 1998; Monteiro et al., 2005). Considering the close link between phosphoinositide (PI)-specific PLC (PI-PLC), $InsP_3$ production, and Ca^{2+} release, it has been speculated that a PI-PLC should be active in regulating the Ca^{2+} dynamics that are known to drive tip growth in pollen tubes (Trewavas and Malhó, 1997; Holdaway-Clarke and Hepler, 2003). There are also some indications of PLC action in the self-incompatibility mechanism in poppy (*Papaver rhoeas*) pollen (Franklin-Tong et al., 1996), and inositol phosphates, such as $InsP_3$ and inositol 1,3,4,5-tetrakisphosphate, do affect pollen tube growth (Zonia et al., 2002; Monteiro et al., 2005). In addition to a potential role for $InsP_3$ in regulating cytosolic Ca^{2+} dynamics, $PtdInsP_2$ compartmentalization mediated by PI-PLC has also been proposed to be important for the control of pollen tube elongation (Kost et al., 1999). $PtdInsP_2$ is thought to interact with many of the actin binding proteins that may regulate growth-related cytoskeletal dynamics in the growing tube (e.g., ADF and profilin) (Yang et al., 1993; Drøbak et al., 1994; Gungabissoon et al., 1998; Chen et al., 2003). Vesicle trafficking has also been reported to be sensitive to PtdIns levels in plant cells (Matsuoka

[1] Current address: UMR de Génétique Végétale, Institut National de la Recherche Agronomique, Centre National de la Recherche Scientifique, Université Paris-Sud, Institut National Agronomique Paris-Grignon, Ferme du Moulon, 91190 Gif-sur-Yvette, France.
[2] Current address: Department of Biology, Pennsylvania State University, University Park, PA 16802.
[3] To whom correspondence should be addressed. E-mail sxg12@psu.edu; fax 814-865-9131.
The author responsible for distribution of materials integral to the findings presented in this article in accordance with the policy described in the Instructions for Authors (www.plantcell.org) is: Simon Gilroy (sxg12@psu.edu).
[W] Online version contains Web-only data.
Article, publication date, and citation information can be found at www.plantcell.org/cgi/doi/10.1105/tpc.106.041582.

et al., 1995; Kim et al., 2001). Thus, PI-PLCs could exert control in tip growth not only through control of $InsP_3$-gated Ca^{2+} fluxes but also by altering the spectrum of PI lipids in the tube apex that in turn likely regulate the tip growth machinery.

However, in all of these cases, the precise molecular identity of the relevant pollen-expressed phospholipases has not been determined. Similarly, whether the lipid turnover events represent specific PLC action is unknown. For example, both $PtdInsP_2$-dependent and -independent phospholipase D activities have been detected in pollen, and phospholipase D activity does appear to be required for pollen tube elongation (Potocky et al., 2003; Monteiro et al., 2005).

Therefore, we have cloned the cDNA for a PI-PLC of *Petunia inflata*, named Pet PLC1, that is expressed in growing pollen tubes. We then assessed the role of this enzyme in regulating pollen tube growth. We report that Pet PLC1 is involved in stabilizing the apical Ca^{2+} gradient normally required for directed tip growth and in maintaining actin dynamics associated with growth. Interfering with Pet PLC1 action alters pollen tube elongation, causing delocalization of the apical Ca^{2+} gradient, disruption of actin structure, and swelling of the apex of the tube. These phenotypic effects can be suppressed by depolymerizing actin with low levels of latrunculin B (Lat B), suggesting that Pet PLC1 may play a role in modulating actin action in tip growth. We also report that Pet PLC1 is enriched in the apical plasma membrane of the pollen tube and that the intensity of this localization is dependent upon the growth status of the tube. These data implicate Pet PLC1 as an important element of the cellular machinery allowing pollen tube extension.

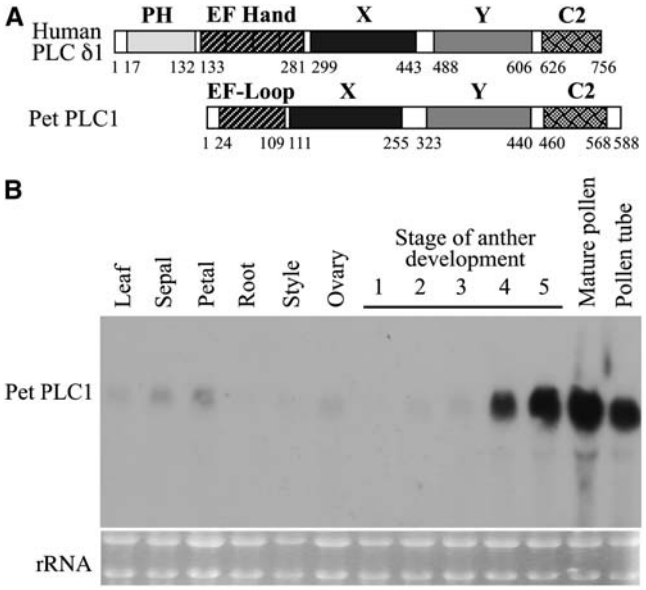

Figure 1. Pet *PLC1* Encodes a PLC Predominantly Expressed in Pollen/Pollen Tubes.

(A) Scheme of the domain structures of Pet PLC1 and human PLC δ1. An alignment of the complete sequences of Pet PLC1 and homologous *Arabidopsis* PLCs, At PLC2 and At PLC4, is shown in Supplemental Figure 1 online. The EF-loop and the C2 domain contain motifs likely involved in the regulation of enzyme activity by Ca^{2+} and/or lipids.

(B) RNA gel blot analysis of the expression of Pet *PLC1*. Total *Petunia* RNA (20 μg) was isolated from each of the tissues indicated and from pollen and pollen tubes and loaded in each lane, and the blot was hybridized with radiolabeled Pet *PLC1* cDNA. Ethidium bromide staining of the gel used for blotting shows rRNA bands as a loading control. Stages of anther development correspond to developing microspores in the tetrad configuration (1), free uninucleate microspores (2), binucleate microspores (3), microspores that have completed mitotic division (4), and open flowers containing mature pollen (5).

RESULTS

A PI-PLC Is Present in Actively Growing *Petunia* Pollen Tubes and Supports Tube Growth

We first isolated candidate cDNAs for PI-PLCs from a pollen/pollen tube cDNA library of *P. inflata* using as a probe a PCR fragment containing the coding regions for the highly conserved X and Y catalytic domains of At *PLC2* of *Arabidopsis thaliana* (Rebecchi and Pentyala, 2000; Wang, 2001). Only one class of clones was isolated in these screens, and the clone containing the longest insert encoded a full-length PLC, which we named Pet PLC1. As with all plant PLCs described to date, compared with the sequences of the animal PLC family members, Pet PLC1 is most similar to the mammalian δ isoform. Figure 1A shows that Pet PLC1, like other plant PLCs, contains a C2 Ca^{2+}/phospholipid binding domain (Kopka et al., 1998), the conserved X and Y catalytic domains, and a region homologous with the second loop of the Ca^{2+} binding EF hand of PLC δ, the so-called EF-loop (Otterhag et al., 2001). However, like other plant PLCs, Pet PLC1 also lacks the $PtdInsP_2$ binding (PH) domain involved in membrane targeting and processive catalysis found in nearly all animal PLCs (Paterson et al., 1995; Essen et al., 1996; Katan and Williams, 1997). An alignment of the deduced amino acid sequences of Pet PLC1 and its most closely related *Arabidopsis* homolog, At PLC2, is shown in Supplemental Figure 1 online.

RNA gel blot analysis indicated that Pet *PLC1* was expressed predominantly in anther/pollen and was expressed at very low levels, if at all, in all other tissues examined (Figure 1B). During anther development, the Pet *PLC1* transcript was first detected at stage 4, approximately the time when microspores are undergoing mitosis (ss., 1994), peaked with pollen maturation, and was maintained during pollen tube growth (Figure 1B).

Pet PLC1 Is Targeted to the Apical Plasma Membrane

There appear to be two major classes of PI-PLCs in plants (Drøbak, 1992). One class is principally cytosolic, requiring millimolar Ca^{2+} concentrations for activity and preferentially using PtdIns as a substrate, whereas the other is membrane-bound, requires micromolar Ca^{2+} concentrations, and preferentially uses $PtdInsP_2$ and phosphatidylinositol 4-phosphate as its substrates. Mung bean (*Vigna radiata*) PLC3 has been tentatively localized to the plasma membrane when heterologously expressed in *Arabidopsis* suspension culture cells, providing a molecular candidate for one membrane-bound enzyme (Kim

et al., 2004). Several putative regulators of the tip growth machinery in pollen tubes (e.g., the Rop monomeric G-proteins and their interacting proteins [Wu et al., 2000; Yang, 2002]) have also been shown to localize to the apical membrane of the tube. Therefore, we sought to characterize the localization and PI-PLC activity of Pet PLC1 to ascertain whether we could place it in one of these broad subcellular classes.

We fused green fluorescent protein (GFP) to the N terminus of Pet PLC1 and used biolistic transformation to transiently express this fusion protein in pollen and pollen tubes under the control of the *LAT52* promoter. Expression of this construct caused no detectable growth-related phenotype in >150 pollen tubes examined. As shown in Figure 2A, a fraction of GFP:Pet PLC1 was associated with the apical cytoplasm, with a fraction targeted to the apical plasma membrane, a localization not seen with soluble GFP (Figure 2B). This membrane targeting led us to speculate that the localization of the enzyme might be involved in regulating tip growth, as proposed for Rops (Gu et al., 2005). Therefore, we characterized the relationship of the GFP:Pet PLC1 localization to phases of rapid elongation and slowing of growth characteristic of pollen tube elongation. Although pollen tubes from species such as lily (*Lilium davidii*) show regular oscillatory growth when grown in vitro (Holdaway-Clarke and Hepler, 2003), pollen tubes of *Petunia* and *Nicotiana* do not exhibit this characteristic of clear, regular pulsatile growth (Pierson et al., 1995; Geitmann et al., 1996; Geitmann 1997; Geitmann and Cresti, 1998; P.E. Dowd, T.-h. Kao, and S. Gilroy, unpublished data). *Petunia* pollen tubes, however, do show phases of rapid elongation interspersed with periods of slowing and cessation of growth, although these occur with less predictable periodicity (see Supplemental Movie 1 online). Therefore, we followed GFP:Pet PLC1 localization as the pollen tubes went through these phases of elongation. Figure 2C shows frames taken from a typical movie of such growth (see Supplemental Movie 1 online). During periods of elongation (0 to 5:00 in Figure 2C), GFP:Pet PLC1 was localized to the lateral plasma membrane just behind the growing tip, with depletion of plasma membrane localization in regions showing rapid expansion. However, during periods of reduced elongation/growth arrest, the apical localization became more prominent around the entire apex of the tube (7:12 to 8:12 in Figure 2C). When growth resumed (12:48 in Figure 2C), this clear apical localization was reduced at the region where the tip started to expand.

To further characterize the localization of GFP:Pet PLC1, we imaged the expression of GFP:Pet PLC1 and labeled the growing pollen tubes with the fluorescent dye FM 4-64 (Figure 2D). FM 4-64 has been used extensively in pollen tubes to visualize both the plasma membrane and a pool of vesicles that form an inverted cone centered on the growing tip (Parton et al., 2001). These vesicles are thought to represent the endocytotic pool associated with membrane recovery during the massive exocytosis associated with tip growth (Parton et al., 2001; de Graaf et al., 2005; Monteiro et al., 2005). We observed that, although GFP:Pet PLC1 did not colocalize with FM 4-64 staining in the shank or more subapical regions of the growing pollen tube, there was substantial overlap in localization in the apex, with apical plasma membrane and the vesicle cone both being costained (arrows in Figure 2D and Supplemental Movie 2

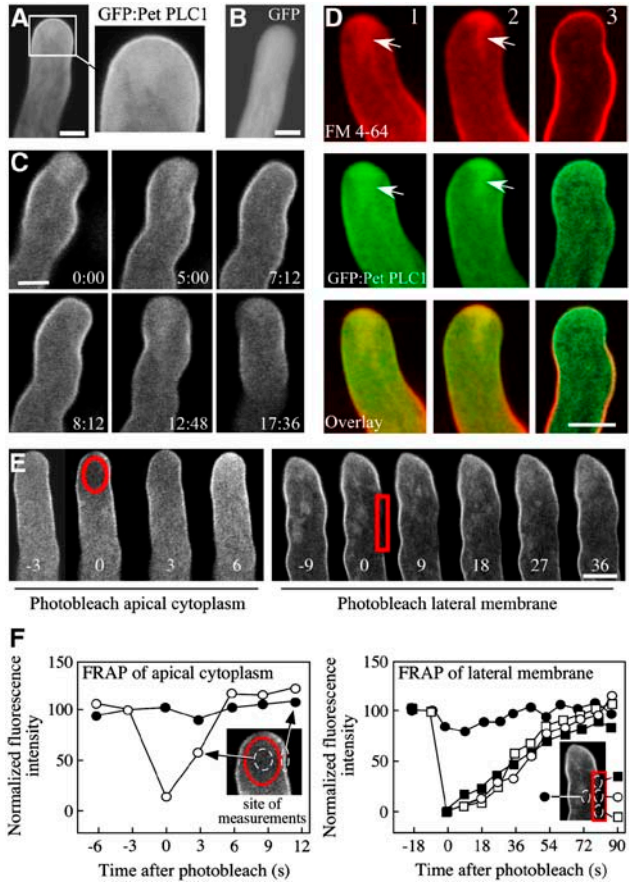

Figure 2. Localization of Pet PLC1 in Growing Pollen Tubes.

(A) and **(B)** Pollen was biolistically transformed with constructs encoding a GFP:Pet PLC1 fusion protein **(A)** or soluble GFP as a control **(B)**. Note the localization of GFP:Pet PLC1 to the apical plasma membrane, which is magnified in the boxed inset. Images represent an extended depth of focus of 20 confocal optical sections 0.5 μm apart. The images shown are representatives of those obtained from >100 individual pollen tubes.

(C) Time course of GFP:Pet PLC1 localization. Single midplane optical sections were taken at the indicated times (minutes). The series of images shown is representative of >30 individual movies.

(D) Colocalization of FM 4-64 and GFP:Pet PLC1. Representative images are of growing (1 and 2) and nongrowing (3) pollen tubes showing the colocalization of FM 4-64 and GFP:Pet PLC1 signals and the overlay of these images. Colocalizing pixels are coded yellow in the overlay images. Note the colocalization in the inverted cone of FM 4-64–stained vesicles (arrows). Controls for bleed through of FM 4-64 or GFP:Pet PLC1 labeling alone indicated no contamination of FM 4-64 signal in the GFP:Pet PLC1 image and vice versa.

(E) FRAP analysis of pollen tubes expressing GFP:Pet PLC1. Numbers represent times (seconds) after photobleaching, which was performed in the areas indicated in red. The series of images shown are representative of more than nine separate experiments. Bars in **(A)** to **(E)** = 10 μm.

(F) Quantitative analysis of photobleaching recovery. Fluorescence intensity was monitored in the indicated regions (dashed boxes in the insets) before and after photobleaching of the regions defined by the red boxes. Intensities were normalized to the measurement made directly before bleaching. Note that all regions of the lateral membrane recover with similar kinetics, suggesting that the flow of unbleached GFP:Pet PLC1 occurs not only from insertion at the tip of the pollen tube.

online). In nongrowing tubes, there was no evidence of the vesicle cone by either GFP:Pet PLC1 or FM 4-64 staining, which uniformly stained the plasma membrane (Figure 2D; see Supplemental Movie 3 online), consistent with the proposed role of the FM 4-64 staining vesicle pool in active tip growth.

We next used fluorescence recovery after photobleaching (FRAP) analysis to define whether this membrane localization of GFP:Pet PLC1 was dynamic. We photobleached the GFP:Pet PLC1 associated with the lateral plasma membrane toward the tube apex and the region of the cytoplasm where the vesicle cone was observed (Figures 2E and 2F). Recovery from photobleaching of the apical cytoplasm occurred within 6 s (Figures 2E and 2F; see Supplemental Movie 4 online), likely by replenishment of unbleached molecules through the vigorous cytoplasmic streaming within the shank of the pollen tube. Fluorescence recovery into bleached areas of the membrane was slower, with full recovery taking ~50 s (Figures 2E and 2F; see Supplemental Movie 5 online). Analysis of fluorescence intensities across the bleached area showed equal recovery rates in the center and periphery of the bleached zone. This observation indicated that unbleached GFP:Pet PLC1 was not moving just into the bleached area from the end closest to the growing tip, suggesting that Pet PLC1 is not only inserted into the membrane at the very apex of the tube (i.e., in the region associated with the FM 4-64 staining vesicle cone). As the cytoplasmic pool of GFP:Pet PLC1 is rapidly redistributed throughout the pollen tube by cytoplasmic streaming, we were unable to robustly determine whether the recovery of Pet PLC1 in the membrane was limited to lateral diffusion of unbleached GFP:Pet PLC1 within the plane of the membrane or via insertion from this cytoplasmic pool. As cytoplasmic streaming does not extend completely to the tip of the tube (Holdaway-Clarke and Hepler, 2003), recovery of the very apical cytoplasmic GFP:Pet PLC1 signal in our FRAP experiments cannot be entirely explained by cytoplasmic streaming.

We next determined that recombinant Pet PLC1 and GFP:Pet PLC1 had associated $PtdInsP_2$-cleaving PLC activity (Figure 3A), whose micromolar Ca^{2+}–dependent activity profile was similar to that detectable in crude microsomal and soluble extracts from pollen tubes (Figure 3B). As noted above, the membrane-bound form of PLC is thought to require micromolar Ca^{2+} concentrations and preferentially use $PtdInsP_2$ and phosphatidylinositol 4-phosphate as its substrates. Thus, the biochemical profile of Pet PLC1 is consistent with the deduction from the GFP imaging described above that this enzyme is likely a membrane-associated $PtdInsP_2$-cleaving enzyme.

Expression of Pet *PLC1-H126A* Disrupts Tip Growth

As Pet PLC1 showed a localization consistent with a possible role in pollen tube growth, we sought a more direct indication that this enzyme was indeed a candidate for a PLC involved in regulating pollen tube function. Therefore, we used site-directed mutagenesis to change a catalytically required His-126 (in the X domain; see Figure 1A and Supplemental Figure 1 online) to Ala-126 to produce a catalytically inactive protein, named Pet PLC1-H126A. A similar mutation in the human PLC δ1 causes a 20,000-fold decrease in phospholipase activity (Ellis et al., 1998). We first examined whether Pet PLC1-H126A was indeed catalytically inactive by comparing its turnover rate of $PtdInsP_2$ with that of the recombinant wild-type protein. Pet PLC1-H126A showed no detectable $PtdInsP_2$ cleavage under conditions in which both the wild-type enzyme and the GFP:Pet PLC1 were active (Figure 3A).

We reasoned that as Pet PLC1-H126A was catalytically inactive, if produced in pollen tubes it might compete with the endogenous Pet PLC1 for its regulators, signaling intermediates, and/or targeting machinery and so might have a dominant negative–like effect on the endogenous enzyme. Thus, we used biolistic transformation to transiently express Pet *PLC1-H126A* (under the control of the pollen-expressed *LAT52* promoter of tomato) (Twell et al., 1990), along with soluble GFP, in pollen. GFP expression was used to identify transformants and was driven by a separate *LAT52* promoter present in the same plasmid as the test construct. This dual construct/single vector approach allowed us to use the expression of GFP in different pollen grains/tubes to more reliably assess the likely expression of a particular test construct. Expression of Pet *PLC1-H126A* led to the arrest of tube growth and swelling of the pollen tube tip (Figure 3C). We also used biolistic transformation to express wild-type Pet *PLC1* under the control of the *LAT52* promoter; however, no alteration of pollen tube growth was observed ($n > 50$, at least three separate experiments; data not shown). We hypothesize that the overexpressed wild-type protein was being regulated similarly to the endogenous enzyme and so did not alter growth patterns.

Pet *PLC1-H126A* Expression Disrupts the Apical Ca^{2+} Gradient and Actin Dynamics

Tip growth in pollen tubes is known to be associated with a tip-focused Ca^{2+} gradient that is required to drive and orient apical growth (reviewed in Holdaway-Clarke and Hepler, 2003). Therefore, we monitored Ca^{2+} gradients in the pollen tubes expressing wild-type Pet *PLC1*, Pet *PLC1-H126A*, or GFP alone to determine their effects on the tip-focused Ca^{2+} gradient (Figure 3D). We observed a Ca^{2+} gradient in untransformed and GFP-expressing pollen tubes, and this gradient was unaltered in tubes that overexpressed wild-type Pet *PLC1* (data not shown). In pollen tubes expressing Pet *PLC1-H126A*, the Ca^{2+} gradient was disrupted, with the region of high Ca^{2+} concentration being much more extensive and filling the entire bulging tip (Figure 3D). This is unlikely to be a feature of high Ca^{2+} always being associated with a bulge at the end of the tube, rather than a more selective effect of Pet *PLC1-H126A*, as other researchers have reported treatments leading to bulging pollen tube tips that are not associated with an increased Ca^{2+} level within the bulge (Cardenas et al., 2005; Gu et al., 2005).

We hypothesized that these effects of Pet PLC1-H126A on normal growth were possibly attributable to competition with the endogenous PLC. Because we had characterized this wild-type enzyme to be localized to the apical plasma membrane (Figure 2A), we tested whether the inactivated enzyme was likewise localized, as expected if it were truly competing with the endogenous PLC for sites on the plasma membrane. Images of GFP:Pet PLC1-H126A taken before it had induced obvious tip

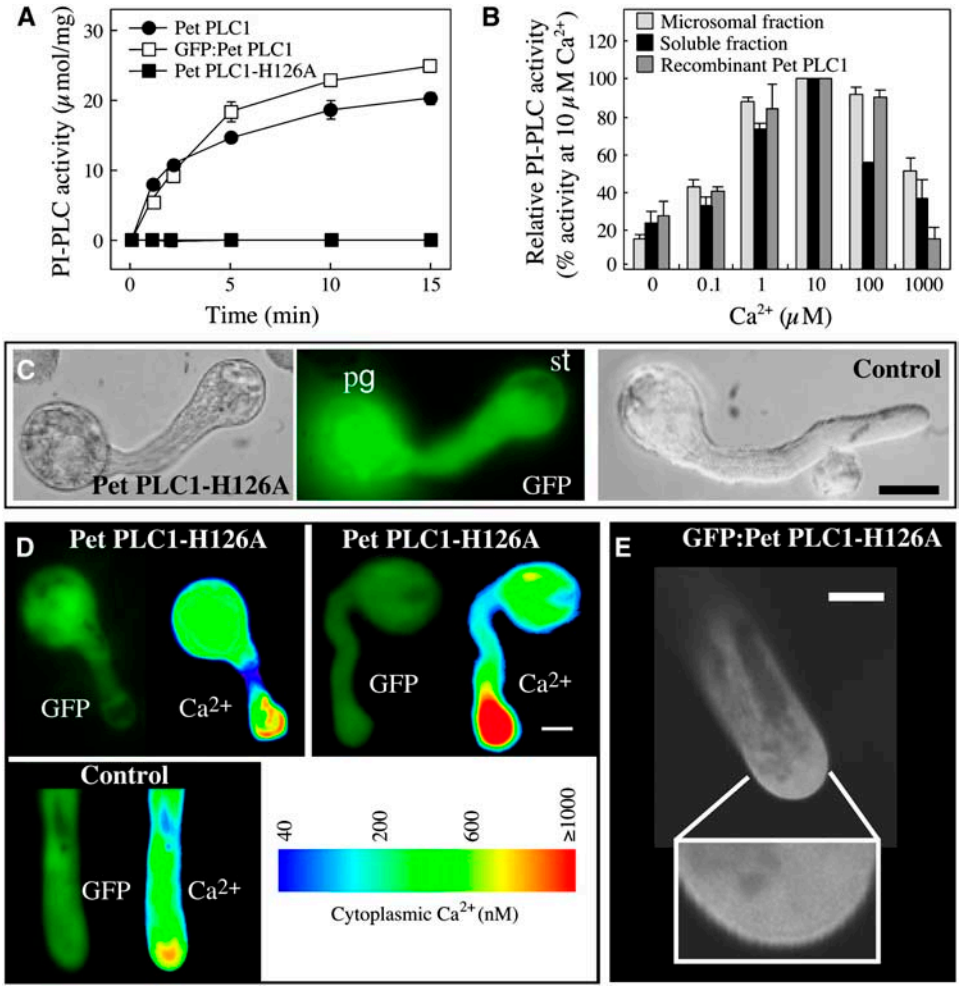

Figure 3. Effect of Pet PLC1-H126A, an Inactive Form of Pet PLC1, on Pollen Tube Growth.

(A) Biochemical assay of recombinant Pet PLC1, GFP:Pet PLC1, and Pet PLC1-H126A. Note that Pet PLC1-H126A has no detectable PI-PLC activity, whereas Pet PLC1 and GFP:Pet PLC1 have nearly identical enzymatic actions (results represent means ± SE; $P > 0.05$, *t* test; $n = 3$).
(B) Production of $InsP_3$ from $PtdInsP_2$ by recombinant Pet PLC1 and by soluble and microsomal fractions of *P. inflata* pollen tubes. Results represent means ± SE ($n = 3$ separate experiments) of PLC activity from the indicated fractions normalized to the activity measured at 10 μM Ca^{2+}.
(C) Morphology of pollen tubes producing both Pet PLC1-H126A and GFP or soluble GFP alone. Left, Pet PLC1-H126A in a bright-field image; middle, GFP fluorescence image showing cotransformed soluble GFP; right, soluble GFP alone used as a control. Note that Pet PLC1-H126A causes arrest of tip growth and apical swelling of the growing tube. pg, pollen grain; st, swollen pollen tube tip. Bar = 20 μm.
(D) Ratio imaging of cytosolic Ca^{2+} in a pollen tube producing GFP alone (control) and two pollen tubes each transiently expressing Pet *PLC1-H126A* and soluble GFP. Pollen tubes were microinjected with the fluorescent Ca^{2+} imaging dye Indo-1-dextran, and Ca^{2+} distribution was calculated by ratio imaging. Ca^{2+} levels have been pseudo-color-coded according to the scale at bottom right. Bar = 20 μm.
(E) Localization of GFP:Pet PLC1-H126A in pollen tubes before induction of bulging. Note the localization to the apical plasma membrane, as also seen for GFP:Pet PLC1. Bar = 10 μm.

swelling showed that this protein was indeed localized to the apical plasma membrane in a pattern very similar to that of the active enzyme, consistent with it acting in a dominant negative manner on the endogenous enzyme (Figure 3E).

Actin is also thought to play a major role in directing normal localized tip growth in pollen tubes (Hepler et al., 2001). Therefore, we coexpressed Pet *PLC1-H126A* with an actin-decorating GFP fusion protein, GFP:mTalin, to assess the effects on actin dynamics in the swollen tube (Figure 4). Similar to the findings reported by others (reviewed in Vidali and Hepler, 2001; Wasteneys and Yang, 2003), in growing pollen tubes used as controls, GFP:mTalin decorated the prominent actin cables running along the shank of the tube, but these cables did not protrude to the very tip of the growing apex (Figure 4A). However, in pollen tubes in which Pet PLC1-H126A had caused an apical swelling, GFP:mTalin decorated a prominent subapical actin band. Such swelling and disruption of actin distribution were suppressed by germinating the pollen grains expressing Pet PLC1-H126A in

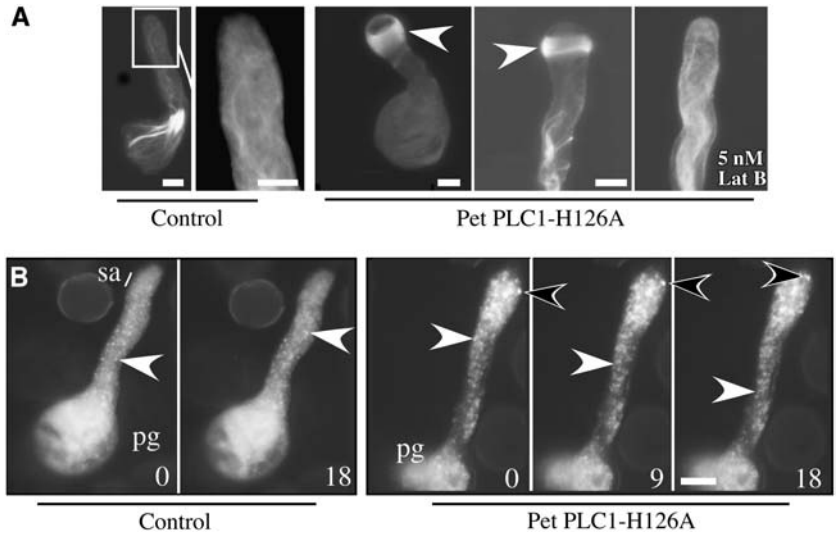

Figure 4. Effect of Pet PLC1-H126A, an Inactive Form of Pet PLC1, on Actin and Golgi Dynamics.

(A) Actin distribution visualized by GFP:mTalin in control pollen tubes and pollen tubes transiently expressing Pet *PLC1-H126A*. Arrowheads point to the subapical actin-rich band that forms in the swollen tip induced by Pet PLC1-H126A. Note that swelling and subapical actin band formation are suppressed by treatment with 5 nM Lat B.

(B) Golgi dynamics in control pollen tubes and those producing Pet PLC1-H126A, as visualized by expression of the Golgi-retained NAG:CFP. Linear tracking of Golgi in the shank of the pollen tube (white arrowheads) is present in both control tubes and tubes producing Pet PLC1-H126A. Note that Golgi are excluded from the extreme tip in the control tube but are accumulated in this region of the Pet PLC1-H126A–producing tube (black arrowheads) from the streaming of Golgi through the swollen tip. pg, pollen grain; sa, subapical region representing maximal travel of Golgi. Numbers represent time in seconds. Images are representatives of those obtained from >20 separate pollen tubes.

Bars = 10 μm.

medium containing 5 nM Lat B (Figure 4A), suggesting that Pet PLC1-H126A may exert its effects on tip growth through disruption of actin dynamics.

Although the subapical actin band was never observed in the GFP:mTalin-expressing control tubes and GFP:mTalin has been used successfully by several groups to monitor the dynamics of actin structure in pollen tubes (Fu et al., 2001; Cardenas et al., 2005), we were concerned that expressing an actin binding protein such as talin could alter the actin dynamics itself and may artifactually implicate Pet PLC1 in modulating the activity of the actin cytoskeleton. Therefore, we also imaged Golgi dynamics to independently confirm likely alterations in actin function induced by Pet PLC1-H126A. Golgi motility is dependent on actin dynamics (Boevink et al., 1998), so monitoring Golgi movements in the pollen tube provided another, albeit indirect, assessment of actin and pollen tube function. We coexpressed a Golgi marker, NAG:CFP, made from fusion of the first 79 amino acids of an *A. thaliana N*-acetylglucosaminyl transferase I to cyan fluorescent protein (CFP) (Dixit and Cyr, 2002), along with Pet *PLC1-H126A*. Importantly, NAG:CFP does not bind to actin and so is unlikely to generate artifacts as a result of potential direct actions on actin dynamics. Golgi are known to be distributed throughout the pollen tube but to be excluded from the secretory vesicle-rich tip (Hepler et al., 2001). In control pollen tubes, NAG:CFP labeled punctate structures characteristic of the Golgi apparatus (Figure 4B), as observed previously by Dixit and Cyr (2002). These structures moved at between 2 and 6 μm/s in the shank of the tube in a linear manner (Figure 4B), consistent with the Golgi tracking along actin microfilaments reported in a variety of cell types (Boevink et al., 1998). This motility was arrested by the addition of 5 μM Lat B, an actin-disrupting drug, again consistent with an actin-based motility system (data not shown). The labeled Golgi were excluded from the very apex of the tube, and once delivered to the cytoplasm just below the tip of the tube, they flowed around this subapical region before returning to linear streaming, back along the length of the tubes' shank (Figure 4B; see Supplemental Movie 6 online). In pollen tubes expressing Pet *PLC1-H126A*, the Golgi dynamics in the tube shank were unaltered relative to controls (Figure 4B; moving in linear streams at 2 to 7 μm/s and qualitatively following similar linear paths as the control). By contrast, at the tube apex, the Golgi now streamed through the end of the tube, protruding to the apex of the swollen tip (see Supplemental Movie 7 online). These observations are consistent with Pet *PLC1-H126A* expression disrupting the actin cytoskeletal organization that prevents Golgi from entering the tube tip. However, the continued Golgi motility in the shank of the tube and through the apex under these circumstances suggests that expression of Pet *PLC1-H126A* did not disrupt all actin-dependent functions within the cell.

Expression of the C2 Domain Alone in Pollen Tubes Phenocopied the Expression of Pet *PLC1-H126A*

The effect of Pet PLC1-H126A on pollen tube growth led us to ask whether the entire protein or a specific domain of Pet PLC1

was responsible for altering tip growth. Therefore, we produced the full-length Pet PLC1 and four different truncated proteins (Figure 5A) in pollen tubes and assessed their effects on growth, Ca^{2+} gradient, actin structure, and Golgi dynamics (Figures 5B to 5E). In addition, we expressed the truncated constructs that retained the X+Y catalytic core in *Escherichia coli* and isolated the recombinant proteins to determine whether they still possessed PI-PLC activity. The truncated protein lacking the EF-loop domain (X+Y+C2), but not the truncated protein lacking the C2 domain (EF+X+Y), retained the catalytic activity (Pet PLC1 = 3.34 ± 0.29, X+Y+C2 = 4.14 ± 1.06, EF+X+Y= 0 μmol·min^{-1}·mg^{-1}). Expressing either the X+Y+C2 or the EF+X+Y construct in pollen tubes did not alter tube morphology or affect the growth-related tip-focused Ca^{2+} gradient (Figure 5B; data not shown). Similarly, expression of the EF-loop construct alone did not alter pollen tube growth or the tip-focused Ca^{2+} gradient (Figure 5B). By contrast, expressing the C2 domain construct alone was able to phenocopy the effects of Pet PLC1-H126A at the level of tube growth. These included swelling of the apex of the tube, alteration of the apical Ca^{2+} gradient (Figure 5C), formation of a subapical actin band (Figure 5D), and protrusion of Golgi to the very tip of the swollen pollen tube (Figure 5E). In a similar manner to Pet *PLC1-H126A* (Figure 4A), when tubes expressing C2 were treated with 5 nM Lat B, no bulging was apparent (Figure 5F).

The similarity in the phenotypes of pollen tubes producing Pet PLC1-H126A and the pollen tubes producing the C2 domain suggested to us that both Pet PLC1-H126A and C2 might affect tube growth by a similar mechanism. In addition, our experiments localizing GFP:Pet PLC1-H126A (Figure 3E) were consistent with this inactivated enzyme binding to similar plasma membrane sites on the wild-type enzyme, raising the possibility that it exerted its effects on growth by displacing the endogenous PLC. Therefore, we coexpressed each of the Pet *PLC1-H126A* and C2 domain constructs with different molar ratios of *GFP*:Pet *PLC1* to determine (1) whether the wild-type protein was mislocalized by expression of these other constructs and (2) whether excess wild-type protein could rescue the effect on pollen tube growth, as would be expected if Pet PLC1-H126A and the C2 domain acted in a dominant negative manner and competed with the endogenous PLC. Indeed, for both Pet PLC1-H126A and C2, GFP:Pet PLC1 was displaced from the apical plasma membrane as the tubes bulged. However, increasing the proportion of competing wild-type protein suppressed both the bulging phenotype and mislocalization (Figure 6). Together, these observations are consistent with both Pet PLC1-H126A and the C2 domain acting in a similar, competitive manner with the endogenous phospholipase.

We reasoned that disruption of PLC localization/function by Pet PLC1-H126A or the C2 domain might alter the levels of PLC's substrate ($PtdInsP_2$) or its products, such as $InsP_3$. Such a change in $PtdInsP_2$ levels could lead to the disruption of the actin cytoskeleton, whereas altering the dynamics of $InsP_3$ might lead to changes in the apical Ca^{2+} gradient, both phenotypes we observed when expressing Pet PLC1-H126A (Figures 3D and 4A) or the C2 domain (Figures 5C and 5F). In the Rop-based signaling network of the pollen tube, phenotypes associated with the alteration of actin dynamics are suppressed by low levels (5 nM) of Lat B (Fu et al., 2001), whereas those related to an altered tip-focused Ca^{2+} gradient can change the Ca^{2+} requirement for pollen germination and growth (Gu et al., 2005). We observed that expression of Pet *PLC1-H126A* or the C2 domain did not alter the requirement for millimolar Ca^{2+} concentrations in the medium for pollen to germinate and undergo tip growth (e.g., 0% germination at 100 μM Ca^{2+}, 70% for Pet *PLC1-H126A*, C2, or control at 3 mM [n > 100 tubes, three separate experiments]). However, germination in 5 nM Lat B did suppress the bulging of the tube tip and the formation of the subapical actin ring in pollen expressing either Pet *PLC1-H126A* (Figure 4A) or the C2 domain (Figure 5F). Addition of 5 nM Lat B to untransformed pollen had no observable effect on germination or growth, whereas addition of ≥1 μM Lat B led to arrested tip growth in both the control and transformed pollen tubes, irrespective of the construct being expressed (data not shown).

These results suggested to us that Pet PLC1-H126A might affect tip growth by altering $PtdInsP_2$ levels, thus affecting actin dynamics. Therefore, we expressed a GFP fusion to the PH domain of human PLC δ1 to investigate whether there were changes in $PtdInsP_2$ levels in the pollen tubes expressing Pet PLC1-H126A. This construct has been used to infer $PtdInsP_2$ localization in animal and plant cells, including tip-growing cells such as root hairs (Vincent et al., 2005) and pollen tubes (Kost et al., 1999). We observed that, as reported by Kost et al. (1999), high expression of this construct led to growth arrest in pollen tubes (data not shown). However, at lower expression levels (as inferred from the brightness of GFP), growth was sustained, and we observed that in growing pollen tubes the GFP:PH signal appeared higher toward the growing apex, whereas in nongrowing tubes this labeling was uniform throughout the pollen tube (Figures 7A and 7B). This membrane localization suggested that GFP:PH selectively labeled the membrane lipid (i.e., $PtdInsP_2$) as opposed to its other potential reported ligand, soluble $InsP_3$ (Lemmon et al., 1995). When the intensity and distribution of GFP:PH fluorescence were compared with those of colabeling with FM 4-64, the two signals did not mirror each other, indicating that GFP:PH did not merely reflect the distribution of membranous material at the apex that is associated with growth. Thus, GFP:PH signal appeared locally enhanced in the regions where tip growth occurred (Figures 7A and 7B; see Supplemental Movies 8 and 9 online). In tubes induced to bulge by the expression of Pet PLC1-H126A or the C2 domain alone, GFP:PH decorated the entire plasma membrane of the bulge.

DISCUSSION

Apical growth in plants is associated with a tip-focused Ca^{2+} gradient that is thought to drive and direct growth. Plant cells usually maintain a cytosolic Ca^{2+} concentration of ~100 nM, but a concentration of several micromolar is found in the apical few micrometers of tip-growing cells (reviewed in Holdaway-Clarke and Hepler, 2003). Although influx of Ca^{2+} through apically localized, possibly stretch-activated (Dutta and Robinson, 2004) Ca^{2+}-permeable channels is likely to support some of this gradient, how the gradient is controlled remains largely unknown. Similarly, a fine network of actin is thought to be intimately involved in the organization and function of the apical

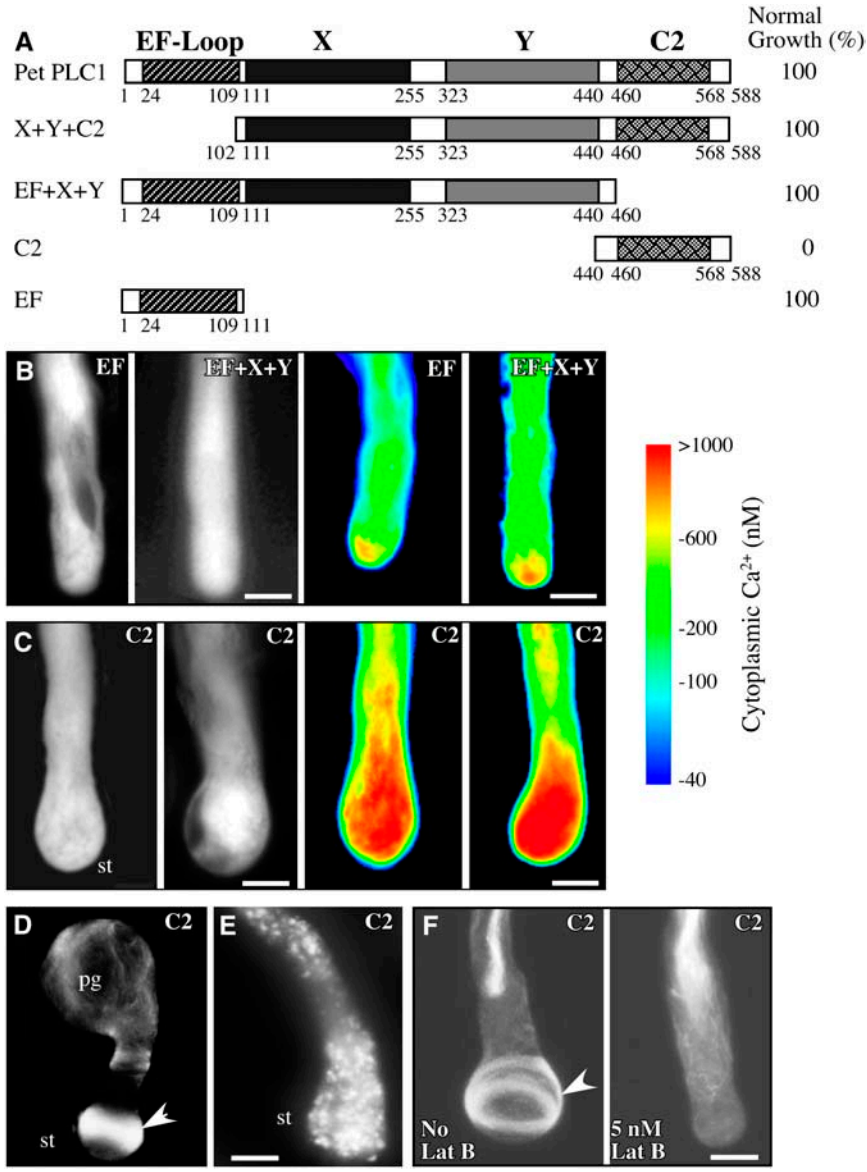

Figure 5. Effects of the Expression of Various Truncated Forms of Pet PLC1 on Pollen Tube Growth.

(A) Schemes of the full-length and four truncated constructs of Pet PLC1, quantifying the effect of overproducing the full-length protein or producing each truncated protein on pollen tube morphology. The morphology of at least 80 pollen tubes that produced GFP from at least three independent experiments was examined for each construct.

(B) Effects of producing the EF domain alone or an EF+X+Y–truncated version of Pet PLC1 on tip growth and Ca^{2+} levels. Each construct was cobombarded with *pLAT52*:*GFP*, and the pollen tubes shown were imaged for GFP fluorescence (left two panels). The same pollen tubes were also imaged for cytosolic Ca^{2+} after they had been microinjected with the fluorescent Ca^{2+} imaging dye Indo-1-dextran (right two panels). The Ca^{2+} distribution was calculated by ratio imaging, and Ca^{2+} levels have been pseudo-color-coded according to the scale at right. Note that neither construct causes tip bulging or detectable alteration in the tip-focused Ca^{2+} gradient.

(C) Effect of expressing the C2 domain alone. Two separate pollen tubes were imaged for GFP fluorescence (left two panels) and Ca^{2+} (right two panels), as described for **(B)**. Note that this construct causes apical swelling of the growing tube and expansion of the tip-focused Ca^{2+} gradient to fill the swollen apex.

(D) Actin distribution visualized by GFP:mTalin in a pollen tube producing the C2 domain alone. The arrowhead points to the subapical actin-rich band that forms in the swollen tip (st). pg, pollen grain.

(E) Golgi dynamics of a pollen tube producing the C2 domain alone as visualized by expression of the Golgi-retained NAG:CFP. Note that Golgi move to the extreme tip of the tube.

(F) Actin distribution visualized by GFP:mTalin in pollen tubes producing the C2 domain with or without 5 nM Lat B added at pollen tube germination. The images shown are representatives of those obtained from >10 separate pollen tubes (**[C]**, **[E]**, and **[F]**), >20 separate pollen tubes **(D)**, or >50 separate pollen tubes **(B)**. Bars = 10 μm.

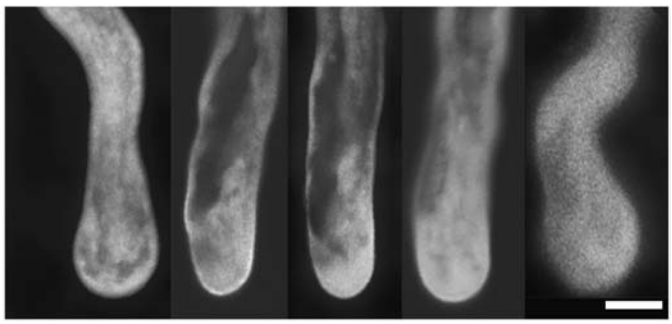

GFP:Pet PLC1:	1	2	2	2	1
Pet PLC1-H126A:	1	1	-	-	-
C2 domain only:	-	-	-	1	1

Figure 6. Effects of Increasing the Relative Amounts of GFP:Pet PLC1 to Pet PLC1-H126A or the C2 Domain on Pollen Tube Morphology and GFP:Pet PLC1 Localization.

Numbers represent amounts of the construct DNA used in each bombardment relative to the 2 μg per bombardment of either the Pet PLC1-H126A or the C2 domain construct. Note that as the relative amount of wild-type GFP:Pet PLC1 is increased, the swelling of the tip induced by either the C2 domain or Pet PLC1-H126A is reduced. Similarly, as wild-type GFP:Pet PLC1 levels are increased, the localization of Pet PLC1 to the apical plasma membrane becomes more pronounced. Images are representative of >30 tubes per treatment from three independent experiments. Bar = 10 μm.

secretory machinery driving tip growth, yet the regulators that maintain this actin network are far from clear. In this work, we have shown that Pet PLC1 appears to be involved in the cellular machinery that regulates the tip-focused Ca^{2+} gradient, actin dynamics, and localized apical secretion.

PI-PLC controls the levels of $PtdInsP_2$ (its substrate) and $InsP_3$ (its cleavage product), both of which are strong candidates to regulate tip growth. Thus, in eukaryotic cells, $InsP_3$ is well defined as triggering Ca^{2+} release from internal stores with, for example, PLC activation being proposed to link signals such as abscisic acid to Ca^{2+}-trigerred stomatal closure through the production of IP_3 (Hunt et al., 2003; Mills et al., 2004). As a tip-focused Ca^{2+} gradient is thought to drive pollen tube growth, regulation of $InsP_3$ levels would be an obvious way for Pet PLC1 to influence tip growth dynamics. Release of $InsP_3$ has been shown to disrupt pollen tube elongation (Monteiro et al., 2005), consistent with a role for $InsP_3$ in sustaining pollen tube function. However, current evidence suggests that Ca^{2+} influx at the plasma membrane supports the Ca^{2+} gradient, rather than the release from internal stores that would likely be triggered by $InsP_3$ (Holdaway-Clarke and Hepler, 2003). In addition, when $InsP_3$ was released in pollen tubes, Ca^{2+} changes were observed around the vegetative nucleus and subapical region, with either no specific alteration or an eventual dissipation in the tip-focused gradient (Franklin-Tong et al., 1996; Monteiro et al., 2005). Thus, it is possible that features other than $InsP_3$ production and its subsequent gating of Ca^{2+} fluxes may be important for PLC's regulatory role in the pollen tube. Unfortunately, the limited sensitivity of the available GFP sensor for imaging $InsP_3$ (Tanimura et al., 2004) has precluded direct analysis of its dynamics at the growing tip.

However, our findings that as Pet PLC1 localization changes, so does $PtdInsP_2$ accumulation (as inferred from changes in GFP:PH accumulation) (Figure 7A), and that expressing an inactivated Pet PLC1 alters $PtdInsP_2$ levels are consistent with the regulation of $PtdInsP_2$ levels by Pet PLC1 being a key component in regulating tip growth. Indeed, Monteiro et al. (2005) have reported that activation of caged $PtdInsP_2$ in pollen tubes triggers the disruption of tip growth, similar to our finding using the disruption of Pet PLC1. We observed that even in nongrowing pollen tubes, GFP:PH labeled the membrane, whereas in growing tubes, this probe (and, by inference, the $PtdInsP_2$ to which it is bound) exhibited an enhanced accumulation in the growing apex. Thus, it seems likely that it is not simply the presence of $PtdInsP_2$ in the plasma membrane that is important for specifying growth but the gradient of accumulation that may define the growth point. The depletion of Pet PLC1 at the growing point would provide one mechanism to support this localized $PtdInsP_2$ accumulation. Indeed, a possible role of PLC in the control of $PtdInsP_2$ dynamics was postulated previously by Kost et al. (1999), and this lipid has been shown to have regulatory effects on cytoskeletal structure, for example, through well-characterized interactions with the actin-severing protein cofilin (van Rheenen and Jalink, 2002; Chen et al., 2003) and the G-actin binding protein profilin (Drøbak et al., 1994; Kovar et al., 2001), through possible control of Ca^{2+} channel gating (Wu et al., 2002), and through regulation of other lipid mediators of tip growth, such as phosphatidic acid generation (Potocky et al., 2003; Monteiro et al., 2005).

To further address whether Pet PLC1 might act through pathways related to Ca^{2+} influx or actin dynamics, we assessed whether the phenotypic effects of the inactive form of Pet PLC1, Pet PLC1-H126A, could be suppressed or enhanced by alterations in extracellular Ca^{2+} levels or by low levels of the actin-depolymerizing drug Lat B. Both of these treatments are known to affect the severity of the pollen phenotypes relating to disruption of the Rop regulatory network, and they have been used to

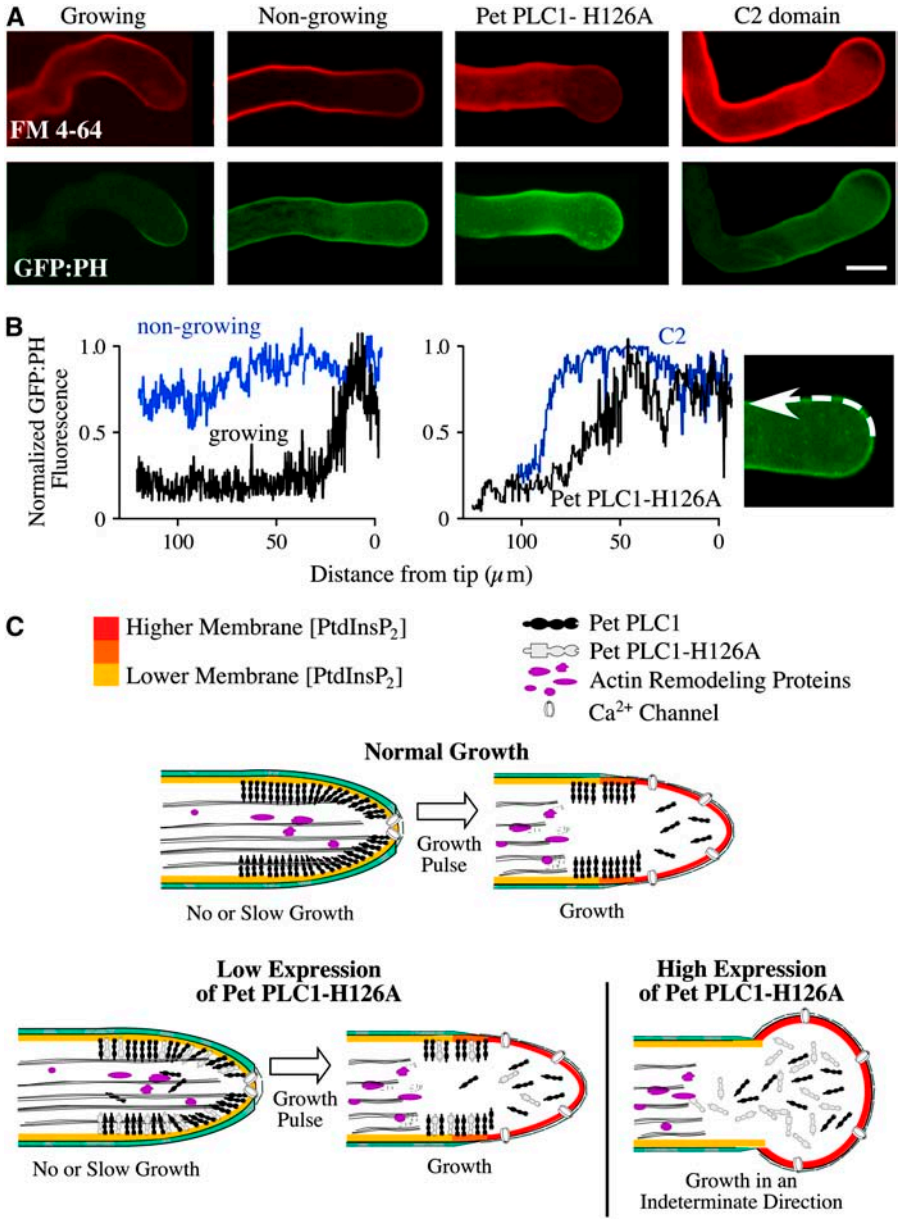

Figure 7. Localization of FM 4-64 and GFP:PH in Growing and Nongrowing Pollen Tubes.

(A) Pollen tubes expressing the GFP:PH construct were stained with 5 μM FM 4-64, and midplane confocal images were taken from pollen tubes that were actively elongating (growing), had arrested in elongation (nongrowing), or were expressing Pet *PLC1-H126A* or the C2 domain construct. Results are representative of >30 tubes from at least three separate experiments. Bar = 10 μm.

(B) Intensity profiles along the plasma membrane of GFP:PH signal normalized to the highest intensity pixel in each transect. One-pixel-wide transects were traced along the plasma membrane according to the image at right, and pixel intensities were recorded using Zeiss LSM 510 image-analysis software. Transects are representative of at least five separate measurements.

(C) Model of the role of Pet PLC1 and $PtdInsP_2$ in tip growth. When growth is slow, Pet PLC1 accumulates on the apical plasma membrane, cleaving $PtdInsP_2$; consequently, levels of apical $PtdInsP_2$ are low. Upon growth, Pet PLC1 leaves the plasma membrane, likely accumulating on the FM 4-64–stained endocytotic/exocytotic vesicle pool at the tip. $PtdInsP_2$ increases in the tube apex, sustaining growth through regulation of membrane dynamics and/or alterations in cytoskeletal structure. Expression of high levels of the inactive Pet PLC-H126A displaces endogenous PLC, leading to increased $PtdInsP_2$ throughout the tip and unrestricted, depolarized growth.

infer a role for Rop-associated proteins in Ca^{2+}- and actin-dependent regulatory events, respectively (Gu et al., 2005). Our observations that tip bulging and the generation of a subapical actin band caused by the expression of either Pet *PLC1-H126A* or the C2 domain of Pet PLC1 were unaltered by changes in extracellular Ca^{2+} levels, but were suppressed by Lat B (Figures 4A and 5D), suggest that these disruptions in growth are likely associated with altered actin dynamics rather than directly with changes in Ca^{2+} fluxes. These findings again highlight the possible role of PLC in regulating the levels of its substrate, $PtdInsP_2$.

Expression of the C2 Ca^{2+}/phospholipid binding domain of Pet PLC1 alone phenocopied the expression of Pet *PLC1-H126A*, whereas the other truncation constructs we tested had no detectable effect on tip growth (Figure 5). One explanation for these observations is that the C2 domain interferes with the regulation of the endogenous enzyme through its own C2 domain. It is also possible that the exogenous C2 displaces Pet PLC1 and/or other C2 domain–containing proteins from the apical plasma membrane. Because we observed that expression of the C2 domain alone can alter the membrane association of the endogenous Pet PLC1 (Figure 6B), the C2 domain may be an important determinant of the membrane localization and specificity of activity of the wild-type enzyme. Thus, correct targeting of Pet PLC1 may be a critical component of its ability to participate correctly in the tip growth machinery. Interestingly, the C2 domain from *Arabidopsis* phospholipase Dβ shows inhibition of $PtdIns_2$ and enhancement of phosphatidylcholine binding at micromolar Ca^{2+} levels (Zheng et al., 2000, 2002; Pappan et al., 2004). These observations raise the possibility that the C2 domain of Pet PLC1 might act to target this enzyme to the apical or lateral membrane of the pollen tube dependent on cytosolic Ca^{2+} level. In this scenario, the increased levels of cytosolic Ca^{2+} found in the tip-focused gradient associated with pulses of tube growth would lead to the dissociation of Pet PLC1 from membrane-bound $PtdInsP_2$ at the elongating apex. Indeed, in mammalian cells, the C2 domain of proteins such as protein kinase C is well characterized as mediating such dynamic, Ca^{2+}-dependent membrane associations (Cho, 2001; Evans et al., 2006). At present, we cannot discount the possibility that other C2 domain–containing proteins are also affected by the expression of Pet PLC1's C2 domain. However, the observations that the phenotypes of expressing the C2 alone and expressing Pet *PLC1-H126A* are similar and that both phenotypes are suppressed by Lat B strongly suggest that the phenotypic effects of the C2 are exerted at least in part through the alteration of Pet PLC1-related events.

Even though the EF-loop deletion construct we generated contains a C2 domain and so might be expected to disrupt pollen tube growth similarly to the C2 alone, it did not yield a growth-related phenotype. However, because this truncated Pet PLC1 retains the catalytic activity of PLC (Figure 4A), it may be under controls similar to the full-length native Pet PLC1 and thus be unable to disrupt growth. Interestingly, Otterhag et al. (2001) reported that a similar X+Y+C2 construct of At PLC2 lacks catalytic activity. It is possible that small differences in the deletions around the EF-loop between these two truncated proteins (with the Otterhag construct lacking seven amino acids at its N terminus compared with the construct used in this study; see Supplemental Figure 1 online for details) are responsible for this difference. Another possibility is that the different isoform we analyzed has different requirements for activity. Nonetheless, our results suggest that a functional EF-loop is not an absolute requirement for catalysis in all PLCs.

The existence of a nine-member multigene family of PLC in *A. thaliana* (Mueller-Roeber and Pical, 2002) implies complexity in the spectrum of PLCs responsible for regulatory and housekeeping functions and raises the possibility of developmental and signal-related changes in the expression pattern of each isoform. The *Arabidopsis* PLC to which Pet PLC1 shows the highest amino acid sequence similarity is At PLC2 (69% identity, 82% similarity). However, At *PLC2* exhibits a broader expression pattern (Hirayama et al., 1997; Pina et al., 2005) than Pet *PLC1*, suggesting that At PLC2 may not be a functional homolog of Pet PLC1. Indeed, of the *Arabidopsis* PLCs, only At *PLC4* appears to be highly expressed in germinated pollen (Hunt et al., 2004), and microarray analysis of ungerminated pollen confirms pollen expression of this isoform (Pina et al., 2005). Thus, At PLC4 is a strong candidate for the *Arabidopsis* homolog of Pet PLC1. An alignment of At PLC4 and Pet PLC1 (51% amino acid sequence identity, 69% similarity) is shown in Supplemental Figure 1 online. Two PI-PLCs, named Ld PLC1 and Ld PLC2, have been identified in *L. daviddi* pollen protoplasts (Pan et al., 2005). These proteins exhibit 63 and 65% amino acid identity, respectively (76 and 79% similarity), to Pet PLC1, but at present it is unclear whether either acts as a functional homolog of Pet PLC1 in lily tube elongation.

The mammalian and yeast PLCs are known to be posttranslationally regulated by mechanisms such as G-protein action, translocation to target membranes, and phosphorylation by protein kinases (Rebecchi and Pentyala, 2000; Wang, 2001). Our finding that Pet PLC1 appears to localize to the apical plasma membrane during slow growth, but less distinctly and more in the FM 4-64 staining vesicle cone in growing pollen tubes, supports the idea that translocation/targeting may play a critical role in PLC function, at least in pollen tube growth.

The observations that PI participates in the regulation of vesicle trafficking (De Camilli et al., 1996; Wurmser et al., 1999), of the activity of actin binding proteins (Lassing and Lindberg, 1985; Janmey and Stossel, 1987; Brill et al., 2000), and of voltage-gated Ca^{2+} channels (Wu et al., 2002) are of particular relevance to its potential control of the Ca^{2+}- and actin-dependent secretion that is thought to mediate tip growth of the pollen tube. Our ability to suppress the phenotypes associated with expressing Pet *PLC1-H126A* with low levels of Lat B suggests that this enzyme may play an important role in maintaining actin dynamics, likely through regulation of the $PtdInsP_2$ pool. Consistent with this idea, releasing caged $PtdInsP_2$ in *Agapanthus* pollen tubes has been shown to cause growth perturbation and tip bulging (Monteiro et al., 2005). One model of PLC action consistent with our data is shown in Figure 7C. We hypothesize that a major function of PLC activity is to regulate $PtdInsP_2$ levels in the apical plasma membrane, with increased $PtdInsP_2$ at the tip being associated with growth. Thus, in growing pollen tubes, the apical PLC is depleted at the growing point, perhaps being removed from the plasma membrane into the rapidly cycling FM 4-64 staining pool of vesicles. $PtdInsP_2$ levels, therefore, are locally

increased, supporting growth through either altered membrane properties and/or PI-dependent regulation of actin dynamics. Slow growth is then associated with a reaccumulation of PLC on the plasma membrane, $PtdInsP_2$ turnover, and a loss of growth potential. Expression of Pet PLC1-H126A would then be associated with a displacement of endogenous PLC from the apical plasma membrane, accumulation of $PtdInsP_2$, and an extended region capable of sustaining growth, leading to bulging of the pollen tube tip.

Thus, Pet PLC1 provides the exciting potential to act as a multifunctional integrator of the pollen tube tip growth process at the level of membrane and cytoskeletal function. Defining the targets and regulators that confine this activity to the apical cytoplasm holds the potential to provide significant insight into how the tip growth that is essential to plant fertility is maintained.

METHODS

Assay of PI-PLC Activity

Pollen from 200 *Petunia inflata* flowers was collected in 25 mL of germination medium containing 0.07% (w/v) $Ca(NO_3)_2{\cdot}4H_2O$, 0.02% (w/v) $MgSO_4{\cdot}7H_2O$, 0.01% (w/v) KNO, 0.01% (w/v) H_3BO_3, 0.2% (w/v) sucrose, 15% (w/v) polyethylene glycol 4000, and 20 mM MES, pH 6.0. Pollen was grown for 5 h at 30°C with shaking at 200 rpm. Soluble and membrane fractions were prepared from these pollen tubes essentially as described previously (Drøbak et al., 1994). Briefly, pollen tubes were homogenized in 4 mL of extraction medium (50 mM Bis-Tris propane, MOPS, pH 7.5, 0.33 M sucrose, 5 mM EDTA, 1 mM DTT, 1 mM phenylmethylsulfonyl fluoride, and Complete protease inhibitor cocktail without EDTA [10 μg/mL]; Roche Applied Science) and centrifuged at 10,000*g* for 10 min. The resulting supernatants were centrifuged at 100,000*g* for 30 min. The microsomal pellet was resuspended in 200 μL of 10 mM HEPES/KOH, pH 7.5, 0.33 mM sucrose, 1 mM EDTA, 1 mM DTT, 1 mM phenylmethylsulfonyl fluoride, and Complete protease inhibitor cocktail without EDTA (10 μg/mL). Soluble and membrane fractions were then frozen with liquid N_2 and stored at −80°C. PI-PLC activity was assayed according to Coursol et al. (2000).

Screening of a *P. inflata* Pollen cDNA Library, and RNA Gel Blot Analysis

Floral cDNA was synthesized from total RNA isolated from 10 *Arabidopsis thaliana* flowers by SuperScript II RNase H^- reverse transcriptase (Invitrogen) as described by Skirpan et al. (2001). A 789-bp fragment of At *PLC2*, which included the coding sequences for both the X and Y catalytic domains, was obtained from total floral cDNA by PCR using 5′-GACTGGTAATCAGCTGAGCAG-3′ as the forward primer and 5′-ATTTGAGCACCGTGGCTC-3′ as the reverse primer. The PCR product was cloned into pGEM-T Easy (Promega), radiolabled with ^{32}P using the RTS RadPrime DNA labeling kit (Life Technologies), and used to screen a previously constructed *P. inflata* pollen cDNA library as described by Mu et al. (1994). RNA gel blot analysis was performed as described by Skirpan et al. (2001), except that 20 μg of total RNA was used. The blot was hybridized with a ^{32}P-labeled full-length Pet *PLC1* cDNA clone isolated from the library screen.

Construction of Plasmids for Recombinant Protein Production in *Escherichia coli*

The full-length Pet *PLC1* cDNA clone was used to generate by PCR all of the expression constructs of Pet *PLC1* and its various truncated or mutant versions. Full-length Pet *PLC1* was obtained using 5′-CCATGGCGTCGAAACAGACATA-3′ (primer 1) as the forward primer and 5′-GCGGCCGCTAGATAAATTCAAAACGATA-3′ (primer 2) as the reverse primer. Pet *PLC1-H126A* was amplified by overlapping PCR, using primer 1 (forward primer) and 5′-TAAGAATTGGCGCCCGTGTA-3′ (reverse primer) in one reaction and primer 2 (forward primer) and 5′-TACACGGGCGCCAATTCTTA-3′ (reverse primer) in the other. The DNA fragments generated by the first two reactions were used as a template for a third reaction in which only primer 1 (forward primer) and primer 2 (reverse primer) were used. A truncated Pet *PLC1* containing the coding sequence for the X+Y+C2 domains was made using 5′-CCATGGCGCCTGTCAATCCTAAACGTAAG-3′ as the forward primer and primer 2 as the reverse primer. Another truncated Pet *PLC1* containing the coding sequence for the EF+X+Y domains was amplified using primer 1 as the forward primer and 5′-GCGGCCGCTAATTGTTAGGACCAGCTTTCA-3′ as the reverse primer. The resulting DNA fragment contained at its 3′ end the codon for amino acid residue 446, followed by a stop codon. Each PCR product (flanked by *Nco*I and *Not*I sites included in the primers) was first cloned into pGEM-T Easy. After the sequence had been confirmed, the DNA fragment was released from pGEM-T and cloned into the *Nco*I and *Not*I sites of pRSET B (Invitrogen), which generates 6xHis-tagged recombinant proteins. *GFP*:Pet *PLC1* was generated by first amplifying soluble GFP (sGFP) (Marc et al., 1998) by PCR using the forward primer 5′-CCATGGTGAGCAAGGGCG-3′ and the reverse primer 5′-CCATGGCACCTCCGCCTCCTCCGCCACCTCCGCCTCCCTTGTACAGCTCGTC-3′. This resulted in the deletion of the stop codon of sGFP and the insertion of a linker encoding 10 Gly and 1 Ala residues. The PCR product was then cloned into the *Nco*I site of the full-length Pet *PLC1* in pRSET B.

Bacterial Expression and Protein Purification

Each expression construct was transformed into *E. coli* (BL-21 pLysS). An overnight culture in 1 mL of Luria-Bertani medium was transferred to 250 mL of Luria-Bertani medium, and the culture was grown at 37°C until OD_{600} reached 0.6. Isopropylthio-β-galactoside was then added to a final concentration of 0.5 mM, and the culture was grown at 22°C for 16 h. Bacterial cells were pelleted and frozen at −80°C. All subsequent steps were performed on ice or at 4°C. The pellets were resuspended in 20 mL of sonication buffer (10% [v/v] glycerol, 20 mM Tris-HCl, pH 8, 50 mM NaCl, Complete protease inhibitor cocktail without EDTA, trypsin inhibitor [2 μg/mL], and 0.1% [w/v] lysozyme). The suspension was sonicated, and the lysates were centrifuged for 20 min at 10,000*g*. The supernatant was incubated with 0.5 mL of Talon resin (Clontech) for 2 h with gentle mixing. The resin was poured into a column and washed with 3 volumes of sonication buffer and then with 3 more volumes of sonication buffer containing 10 mM imidazole. Protein was eluted in 300-μL fractions with sonication buffer containing 100 mM imidazole. The purity of each fraction was assessed using 12% (w/v) SDS–polyacrylamide gels.

Construction of Single Expression Plasmids for Transient Expression in Pollen Tubes

All single expression plasmids used for biolistic experiments were constructed in a vector derived from the pBGD vector (James et al., 1996). The 2.8-kb *Sal*I-*Eco*RI fragment, containing the *LAT52* promoter, GUS coding sequence, and NOS terminator, was released from pLAT52-7 (Twell et al., 1990) and inserted into the *Sal*I and *Eco*RI sites of pBGD to generate pLAT-GUS. The GUS sequence and the NOS terminator were then removed by digestion with *Nco*I and *Eco*RI and replaced with the *Nco*I–*Eco*RI fragment from a pUC18 derivative that contains the sGFP coding sequence and the NOS terminator to generate pLAT-GFP. Pet *PLC1* (full length), Pet *PLC1-H126A*, X+Y+C2 (truncated Pet PLC1 lacking the EF-loop), and EF+X+Y (truncated Pet PLC1 lacking the C2

domain) from the *E. coli* expression constructs described above were released from their respective pRSET B constructs and ligated separately into the *Nco*I and *Not*I sites of pLAT-GFP (the GFP fragment was released in the cloning). The EF-loop domain was amplified by PCR using primer 1 (forward primer) and 5′-GCGGCCGCTAATGGTGATCTTACGTTTA-GGA-3′ (reverse primer) to give a fragment starting at the initiation (start) codon within an *Nco*I site and ending at amino acid 102, which is followed by a stop codon and a *Not*I site. The C2 domain was amplified by PCR using forward primer 5′-CCATGGCGAAAGCTGGTCCTAACAATC-3′ and primer 2; this resulted in a fragment with an in-frame ATG within an *Nco*I site and ending at the stop codon and a *Not*I site. Both the EF-loop and C2 fragments were then cloned into the *Nco*I and *Not*I sites of pLAT-GFP as described above.

Construction of GFP:PH

GFP:PH was constructed by PCR of the coding sequence for the PH domain of human PLC δ1 essentially according to Kost et al. (1999), except that the sequence for a seven–amino acid linker (Gly-Gly-Ala-Gly-Ala-Ala-Gly) was inserted between the sequences for GFP and the PH domain. *Aequorea coerulescens* GFP (AcGFP) (Clontech) was amplified using 5′-TTAAGCTTCCATGGTGAGCAAGGGCGC-3′ (primer 1) as the forward primer and 5′-GTCTCCTGCAGCTCCAGCTCCACCCTTGTA-CAGCTCATCCATGCC-3′ as the reverse primer, and the PH domain from a cDNA clone of human PLC δ1 (Open Biosystems) was amplified from the coding sequence corresponding to amino acid residues 2 to 174 using 5′-GGTGGAGCTGGAGCTGCAGGAGACTCGGGCCGGGACTTC-CTG-3′ as the forward primer and 5′-GCGGCCGCTAGATGTTGAGCTC-CTTCAGGAAGTTCTGC-3′ as the reverse primer (primer 2). AcGFP:PH was amplified by primer 1 and primer 2 using both AcGFP and PH domain fragments as templates. This PCR product (flanked by *Hind*III and *Not*I sites included in the primers) was first cloned into pGEM-T Easy. After the sequence had been confirmed, the DNA fragment was released from pGEM-T and cloned into the *Hind*III and *Not*I sites of pLAT-GFP.

Construction of Dual Expression Constructs

Dual expression constructs were made to express both GFP and full-length Pet *PLC1*, or both GFP and Pet *PLC1-H126A*, from the same plasmid. The pLAT-GFP plasmid was used as a template for PCR with the forward primer 5′-AGGCTTCTCGACTCAGAAGGTATTGAG-3′ and the reverse primer 5′-AAGCTTCATGTTTGACAGCTTATCATC-3′. The resulting DNA fragment contained the 0.6-kb *LAT52* promoter, GFP coding sequence, and NOS terminator. This fragment was cloned into pGEM-T Easy, released by digestion with *Eco*RI, and cloned into the *Eco*RI site of the Pet *PLC1* and Pet *PLC1-H126A* single expression constructs, respectively.

Biolistic Transformation

Pollen grains collected from 10 flowers of greenhouse-grown *P. inflata* plants were suspended in 200 μL of germination medium and bombarded with DNA-coated gold particles (1.0 μm diameter) according to Fu et al. (2001). Gold particles (0.5 mg) were coated with 2 μg of plasmid DNA, except for *GFP:mTalin*, for which only 0.8 μg was used. For experiments in which *GFP*:Pet *PLC1* was titrated with different amounts of the C2 domain construct or Pet *PLC1-H126A*, 2 μg of *GFP:*Pet *PLC1* was used and C2 or Pet *PLC1-H126A* was added at between 0.5 and 4 μg. The bombarded pollen grains were incubated at room temperature for 30 min, washed into culture tubes with 1 mL of germination medium, and shaken at 200 rpm at 30°C for 5 h before observation using either a Diaphot 300 epifluorescence microscope (Nikon) or a Zeiss LSM 410 confocal microscope. GFP was imaged using 480 ± 20 nm excitation, 500 nm dichroic mirror, and >510 nm emission (Diaphot) or 488 nm excitation, 488 nm dichroic mirror, and 520 to 560 nm emission (LSM 410). CFP was monitored using 440 ± 20 nm excitation, 460 nm dichroic mirror, and 480 ± 20 nm emission (Diaphot).

Lat B Treatment

To determine the effect of Lat B on the actin organization in *P. inflata* pollen tubes, pollen grains were bombarded with *GFP:mTalin* alone, C2 domain construct + *GFP:mTalin*, or Pet *PLC1-H126A* + *GFP:mTalin*. Lat B (Calbiochem) in a 1 mM stock in DMSO was added to each bombarded sample to a final concentration of 5 nM, with the final DMSO concentration at <0.001% (v/v). DMSO was added to the germination medium of the controls at an equivalent concentration. Pollen tubes were imaged after 4.5 to 5 h as described above.

FM 4-64 Staining, Calcium Measurement, and NAG:CFP Imaging

Pollen tubes were stained according to Parton et al. (2001). FM 4-64 (Molecular Probes) was added to a final concentration of 10 μM into pollen germination medium and visualized after 15 min using a Zeiss LSM 510 Meta microscope (543 nm excitation from a HeNe laser, 488/514/543 nm dichroic mirror, and 560 nm long-pass emission filtration). For measurement of cytosolic Ca^{2+}, pollen tubes of ~50 μm in length were impaled with borosilicate glass micropipettes and pressure-microinjected with Indo-1 conjugated to 10 kD of dextran (Molecular Probes), and Ca^{2+} levels were measured as described previously (Bibikova et al., 1997). To image Golgi distribution, pollen tubes were biolistically transformed with a construct to express NAG:CFP, a protein made from a fusion of the first 79 amino acids of *A. thaliana* *N*-acetylglucosaminyl transferase I to CFP (Dixit and Cyr, 2002). Transformed pollen tubes were imaged using a Diaphot 300 inverted epifluorescence microscope, a CFP filter set (Chroma), and a SenSys cooled CCD camera (Roper Scientific). Individual Golgi were tracked through frames of time-lapse movies (3 s between frames) using IPLabs image-analysis software (Signal Analytics).

Accession Numbers

Sequence data from this article can be found in the GenBank/EMBL databases under the following accession numbers: Pet PLC1, DQ322461; At PLC2, AC074395; At PLC4, NM125257; Ld PLC1, AAW81961; Ld PLC2, AAW81960.

Supplemental Data

The following materials are available in the online version of this article.

Supplemental Figure 1. Amino Acid Sequence Alignment of Pet PLC1 and Two *Arabidopsis* PLCs, At PLC2 and At PLC4.

Supplemental Movie 1. Time Lapse of a Growing Pollen Tube Expressing GFP:Pet PLC1.

Supplemental Movie 2. Time Lapse of a Growing Pollen Tube Expressing GFP:Pet PLC1 and Stained with 5 μM FM 4-64.

Supplemental Movie 3. Time Lapse of a Nongrowing Pollen Tube Expressing GFP:Pet PLC1 and Stained with 5 μM FM 4-64.

Supplemental Movie 4. Fluorescence Recovery after Photobleaching the Cytoplasm in the Tip Region of a Pollen Tube Expressing GFP:Pet PLC1.

Supplemental Movie 5. Fluorescence Recovery after Photobleaching the Membrane along the Shank of a Pollen Tube Expressing GFP:Pet PLC1.

Supplemental Movie 6. Golgi Dynamics in Wild-Type Growing Pollen Tubes.

Supplemental Movie 7. Golgi Dynamics in Pollen Tubes Expressing Pet *PLC1-H126A*.

Supplemental Movie 8. Time Lapse of a Growing Pollen Tube Expressing GFP:PH to Visualize $PtdInsP_2$ Localization.

Supplemental Movie 9. Time Lapse of a Nongrowing Pollen Tube Expressing GFP:PH to Visualize $PtdInsP_2$ Localization.

ACKNOWLEDGMENTS

We thank Sarah Swanson for critical reading of the manuscript, Zhenbiao Yang for providing the GFP:mTalin plasmid, Sheila McCormick for pLAT52-7, Richard Cyr for sGFP and NAG:CFP plasmids, and Anthony Omeis for plant management. This work was supported by a Predoctoral Fellowship for Students with Disabilities from the National Institutes of Health to P.E.D., grants from the USDA and the Pennsylvania State University Innovative Biotechnology Program to S.G. and T.-h.K., and a multiuser equipment grant from the National Science Foundation for the LSM 510 confocal microscope to S.G.

Received February 1, 2006; revised March 17, 2006; accepted April 5, 2006; published April 28, 2006.

REFERENCES

Alexandre, J., Lassalles, J.F., and Kado, R.D. (1990). Opening of Ca^{2+} channels in isolated red beet root vacuole membrane by inositol 1,4,5-trisphosphate. Nature **343,** 567–570.

Bibikova, T.N., Zhigilei, A., and Gilroy, S. (1997). Root hair growth in *Arabidopsis thaliana* is directed by calcium and an endogenous polarity. Planta **203,** 495–505.

Boevink, P., Oparka, K., Santa Cruz, S., Martin, B., Betteridge, A., and Hawes, C. (1998). Stacks on tracks: The plant Golgi apparatus traffics on an actin/ER network. Plant J. **15,** 441–447.

Brill, J.A., Hime, G.R., Scharer-Schuksz, M., and Fuller, M.T. (2000). A phospholipid kinase regulates actin organization and intercellular bridge formation during germline cytokinesis. Development **127,** 3855–3864.

Cardenas, L., Lovy-Wheeler, A., Wilsen, K.L., and Hepler, P.K. (2005). Actin polymerization promotes the reversal of streaming in the apex of pollen tubes. Cell Motil. Cytoskeleton **61,** 112–127.

Chen, C.Y., Cheung, A.Y., and Wu, H.M. (2003). Actin-depolymerizing factor mediates Rac/Rop GTPase–regulated pollen tube growth. Plant Cell **15,** 237–249.

Cheung, A.Y., Chen, C.Y., Tao, L.Z., Andreyeva, T., Twell, D., and Wu, H.M. (2003). Regulation of pollen tube growth by Rac-like GTPases. J. Exp. Bot. **54,** 73–81.

Cho, W. (2001). Membrane targeting by C1 and C2 domains. J. Biol. Chem. **276,** 32407–32410.

Coursol, S., Giglioli-Guivarc'h, N., Vidal, J., and Pierre, J.-N. (2000). An increase in phosphoinositide-specific phospholipase C activity precedes induction of C4 phosphoenolpyruvate carboxylase phosphorylation in illuminated and NH_4Cl-treated protoplasts from *Digitaria sanguinalis*. Plant J. **23,** 497–506.

De Camilli, P., Emr, S.D., McPherson, P.S., and Novick, P. (1996). Phosphoinositides as regulators in membrane traffic. Science **271,** 1533–1539.

de Graaf, B.H.J., Cheung, A.Y., Andreyeva, T., Levasseur, K., Kieliszewski, M., and Wu, H.M. (2005). Rab11 GTPase-regulated membrane trafficking is crucial for tip-focused pollen tube growth in tobacco. Plant Cell **17,** 2564–2579.

de Jong, C.F., Laxalt, A.M., Bargmann, B.O., de Wit, P.J., Joosten, M.H., and Munnik, T. (2004). Phosphatidic acid accumulation is an early response in the Cf-4/Avr4 interaction. Plant J. **39,** 1–12.

Dixit, R., and Cyr, R.J. (2002). Golgi secretion is not required for marking the preprophase band site in cultured tobacco cells. Plant J. **29,** 99–108.

Drøbak, B.K. (1992). The plant phosphoinositide system. Biochem. J. **288,** 697–712.

Drøbak, B.K., Watkins, P.A.C., Valenta, R., Dove, S.K., Lloyd, C.W., and Staiger, C.J. (1994). Inhibition of plant plasma membrane phosphoinositide phospholipase C by the actin-binding protein, profilin. Plant J. **6,** 389–400.

Dutta, R., and Robinson, K.R. (2004). Identification and characterization of stretch-activated ion channels in pollen protoplasts. Plant Physiol. **135,** 1398–1406.

Ellis, M.V., James, S.R., Perisic, O., Downes, C.P., Williams, R.L., and Katan, M. (1998). Catalytic domain of phosphoinositide-specific phospholipase C (PLC). Mutational analysis of residues within the active site and hydrophobic ridge of plcdelta1. J. Biol. Chem. **273,** 11650–11659.

Essen, L.-O., Perisic, O., Cheung, M., Katan, M., and Williams, R.L. (1996). Crystal structure of a mammalian phosphoinositide-specific phospholipase C delta. Nature **380,** 595–602.

Evans, J.H., Murray, D., Leslie, C.C., and Falke, J.J. (2006). Specific translocation of protein kinase Calpha to the plasma membrane requires both Ca^{2+} and PIP2 recognition by its C2 domain. Mol. Biol. Cell **17,** 56–66.

Franklin-Tong, V.E., Drobak, B.K., Allan, A.C., Watkins, P., and Trewavas, A.J. (1996). Growth of pollen tubes of *Papaver rhoeas* is regulated by a slow-moving calcium wave propagated by inositol 1,4,5-trisphosphate. Plant Cell **8,** 1305–1321.

Fu, Y., Wu, G., and Yang, Z. (2001). Rop GTPase-dependent dynamics of tip-localized F-actin controls tip growth in pollen tubes. J. Cell Biol. **152,** 1019–1032.

Fu, Y., and Yang, Z. (2001). Rop GTPase: A master switch of cell polarity development in plants. Trends Plant Sci. **6,** 545–547.

Geitmann, A. (1997). Growth and Formation of the Cell Wall in Pollen Tubes of *Nicotiana tabacum* and *Petunia hybrida*. (Eglesbach, Germany: Hansel-Hohenhausen).

Geitmann, A., and Cresti, M. (1998). Ca^{2+} channels control the rapid expansions in pulsating growth of *Petunia hybrida* pollen tubes. J. Plant Physiol. **152,** 439–447.

Geitmann, A., Li, Y.Q., and Cresti, M. (1996). The role of the cytoskeleton and dictyosome activity in the pulsatory growth of *Nicotiana tabacum* and *Petunia hybrida*. Bot. Acta **109,** 373–381.

Gu, Y., Fu, Y., Dowd, P., Li, S., Vernoud, V., Gilroy, S., and Yang, Z. (2005). A Rho family GTPase controls actin dynamics and tip growth via two counteracting downstream pathways in pollen tubes. J. Cell Biol. **169,** 127–138.

Gungabissoon, R.A., Chang-Jie, J., Drobak, B.K., Maciver, S.K., and Hussy, P.J. (1998). Interaction of maize actin-depolymerising factor with actin and phosphoinositides and its inhibition of plant phospholipase C. Plant J. **16,** 689–696.

Hepler, P.K., Vidali, L., and Cheung, A.Y. (2001). Polarized cell growth in higher plants. Annu. Rev. Cell Dev. Biol. **17,** 159–187.

Hirayama, T., Mitsukawa, N., Shibata, D., and Shinozaki, K. (1997). *AtPLC2*, a gene encoding phosphoinositide-specific phospholipase C, is constitutively expressed in vegetative and floral tissues in *Arabidopsis thaliana*. Plant Mol. Biol. **34,** 175–180.

Holdaway-Clarke, T.L., and Hepler, P.K. (2003). Control of pollen tube growth: Role of ion gradients and fluxes. New Phytol. **159,** 539–563.

Hunt, L., Mills, L.N., Pical, C., Leckie, C.P., Aitken, F.L., Kopka, J., Mueller-Roeber, B., McAinsh, M.R., Hetherington, A.M., and Gray,

J.E. (2003). Phospholipase C is required for the control of stomatal aperture by ABA. Plant J. **34,** 47–55.

Hunt, L., Otterhag, L., Lee, J.C., Lasheen, T., Hunt, J., Seki, M., Shinozaki, K., Sommarin, M., Gilmour, D.J., Pical, C., and Gray, J.E. (2004). Gene-specific expression and calcium activation of *Arabidopsis thaliana* phospholipase C isoforms. New Phytol. **162,** 643–654.

James, P., Halladay, J., and Craig, E.A. (1996). Genomic libraries and a host strain designed for highly efficient two-hybrid selection in yeast. Genetics **144,** 1425–1436.

Janmey, P.A., and Stossel, T.P. (1987). Modulation of gelsolin function by phosphatidylinositol 4,5-bisphosphate. Nature **325,** 362–364.

Katan, M., and Williams, R.L. (1997). Phosphoinositide-specific phospholipase C: Structural basis for catalysis and regulatory interactions. Semin. Cell Dev. Biol. **8,** 287–296.

Kim, D.H., Eu, Y.-J., Yoo, C.M., Kim, Y.-W., Pih, K.T., Jin, J.B., Kim, S.J., Stenmark, H., and Hwang, I. (2001). Trafficking of phosphatidylinositol 3-phosphate from the trans-Golgi network to the lumen of the central vacuole in plant cells. Plant Cell **13,** 287–301.

Kim, Y.J., Kim, J.E., Lee, J.H., Lee, M.H., Jung, H.W., Bahk, Y.Y., Hwang, B.K., Hwang, I., and Kim, W.T. (2004). The Vr-PLC3 gene encodes a putative plasma membrane-localized phosphoinositide-specific phospholipase C whose expression is induced by abiotic stress in mung bean (*Vigna radiata* L.). FEBS Lett. **556,** 127–136.

Kopka, J., Pical, C., Hetherington, A.M., and Muller-Rober, B. (1998). Ca^{2+}/phospholipid-binding (C2) domain in multiple plant proteins: Novel components of the calcium-sensing apparatus. Plant Mol. Biol. **36,** 627–637.

Kost, B., Lemichez, E., Spielhofer, P., Hong, Y., Tolias, K., Carpenter, C., and Chua, N.H. (1999). Rac homologues and compartmentalized phosphatidylinositol 4,5-bisphosphate act in a common pathway to regulate polar pollen tube growth. J. Cell Biol. **145,** 317–330.

Kovar, D.R., Drøbak, B.K., Collings, D.A., and Staiger, C.J. (2001). The characterization of ligand-specific maize (*Zea mays*) profilin mutants. Biochem. J. **358,** 49–57.

Lassing, I., and Lindberg, U. (1985). Specific interaction between phosphatidylinositol 4,5-bisphosphate and profilactin. Nature **314,** 472–474.

Lemmon, M.A., Ferguson, K.M., O'Brian, R., Sigler, P.B., and Schlessinger, J. (1995). Specific and high-affinity binding of inositol phosphates to an isolated pleckstrin homology domain. Proc. Natl. Acad. Sci. USA **92,** 10472–10476.

Malhó, R. (1998). Role of 1,4,5-inositol trisphosphate-induced Ca^{2+} release in pollen tube orientation. Sex. Plant Reprod. **11,** 231–235.

Marc, J., Granger, C.L., Brincat, J., Fisher, D.D., Kao, T.-h., McCubbin, A.G., and Cyr, R.J. (1998). A *GFP-MAP4* reporter gene for visualizing cortical microtubule rearrangements in living epidermal cells. Plant Cell **10,** 1927–1939.

Matsuoka, K., Bassham, D.C., Raikhel, N.V., and Nakamura, K. (1995). Different sensitivity to wortmannin of two vacuolar sorting signals indicates the presence of distinct sorting machineries in tobacco cells. J. Cell Biol. **130,** 1307–1318.

Mills, L.N., Hunt, L., Leckie, C.P., Aitken, F.L., Wentworth, M., McAinsh, M.R., Gray, J.E., and Hetherington, A.M. (2004). The effects of manipulating phospholipase C on guard cell ABA-signalling. J. Exp. Bot. **55,** 199–204.

Monteiro, D., Liu, Q., Lisboa, S., Scherer, G.E., Quader, H., and Malho, R. (2005). Phosphoinositides and phosphatidic acid regulate pollen tube growth and reorientation through modulation of $[Ca^{2+}]_c$ and membrane secretion. J. Exp. Bot. **56,** 1665–1674.

Mu, J.H., Lee, H.-S., and Kao, T.-h. (1994). Characterization of a pollen expressed receptor like kinase gene of *Petunia inflata* and the activity of its encoded kinase. Plant Cell **6,** 709–721.

Mueller-Roeber, B., and Pical, C. (2002). Inositol phospholipid metabolism in Arabidopsis. Characterized and putative isoforms of inositol phospholipid kinase and phosphoinositide-specific phospholipase C. Plant Physiol. **130,** 22–46.

Otterhag, L., Sommarin, M., and Pical, C. (2001). N-terminal EF-hand-like domain is required for phosphoinositide-specific phospholipase C activity in *Arabidopsis thaliana*. FEBS Lett. **497,** 165–170.

Pan, Y.Y., Wang, X., Ma, L.G., and Sun, D.Y. (2005). Characterization of phosphatidylinositol-specific phospholipase C (PI-PLC) from *Lilium daviddi* pollen. Plant Cell Physiol. **46,** 1657–1665.

Pappan, K., Zheng, L., Krishnamoorthi, R., and Wang, X. (2004). Evidence for and characterization of Ca^{2+} binding to the catalytic region of *Arabidopsis thaliana* phospholipase Dbeta. J. Biol. Chem. **279,** 47833–47839.

Parton, R.M., Fischer-Parton, S., Watahiki, M.K., and Trewavas, A.J. (2001). Dynamics of the apical vesicle accumulation and the rate of growth are related in individual pollen tubes. J. Cell Sci. **114,** 2685–2695.

Paterson, H.F., Savopoulos, J.W., Perisic, O., Cheung, R., Ellis, M.V., Williams, R.L., and Katan, M. (1995). Phospholipase C delta 1 requires a pleckstrin homology domain for interaction with the plasma membrane. Biochem. J. **312,** 661–666.

Pierson, E.S., Li, Y.Q., Zhang, H.Q., Willemse, M.T.M., Linskens, H.F., and Cresti, M. (1995). Pulsatory growth of pollen tubes: Investigation of a possible relationship with the periodic distribution of cell wall components. Acta. Bot. Neerl. **44,** 121–128.

Pina, C., Pinto, F., Feijo, J.A., and Becker, J.D. (2005). Gene family analysis of the Arabidopsis pollen transcriptome reveals biological implications for cell growth, division control, and gene expression regulation. Plant Physiol. **138,** 744–756.

Potocky, M., Elias, M., Profotova, B., Novotna, Z., Valentova, O., and Zarsky, V. (2003). Phosphatidic acid produced by phospholipase D is required for tobacco pollen tube growth. Planta **217,** 122–130.

Rebecchi, M.J., and Pentyala, S.N. (2000). Structure, function, and control of phosphoinositide-specific phospholipase C. Physiol. Rev. **80,** 1291–1335.

Skirpan, A.L., McCubbin, A.G., Ishimizu, T., Wang, X., Hu, Y., Dowd, P.E., Ma, H., and Kao, T.-h. (2001). Isolation and characterization of kinase interacting protein 1, a pollen protein that interacts with the kinase domain of PRK1, a receptor-like kinase of petunia. Plant Physiol. **126,** 1480–1492.

Tanimura, A., Nezu, A., Morita, T., Turner, R.J., and Tojyo, Y. (2004). Fluorescent biosensor for quantitative real-time measurements of inositol 1,4,5-trisphosphate in single living cells. J. Biol. Chem. **279,** 38095–38098.

Trewavas, A.J., and Malhó, R. (1997). Signal perception and transduction: The origin of the phenotype. Plant Cell **9,** 1181–1195.

Twell, D., Yamaguchi, J., and McCormick, S. (1990). Pollen-specific gene expression in transgenic plants: Coordinate regulation of two different tomato gene promoters during microsporogenesis. Development **109,** 705–713.

van Rheenen, J., and Jalink, K. (2002). Agonist-induced PIP_2 hydrolysis inhibits cortical actin dynamics: Regulation at a global but not at a micrometer scale. Mol. Biol. Cell **13,** 3257–3267.

Vidali, L., and Hepler, P.K. (2001). Actin and pollen tube growth. Protoplasma **215,** 64–76.

Vincent, P., Chua, M., Nogue, F., Fairbrother, A., Mekeel, H., Xu, Y., Allen, N., Bibikova, T.N., Gilroy, S., and Bankaitis, V.A. (2005). A Sec14p-nodulin domain phosphatidylinositol transfer protein polarizes membrane growth of *Arabidopsis thaliana* root hairs. J. Cell Biol. **168,** 801–812.

Wang, X. (2001). Plant phospholipases. Annu. Rev. Plant Physiol. Plant Mol. Biol. **52,** 211–231.

Wasteneys, G.O., and Yang, Z. (2003). New views on the plant cytoskeleton. Plant Physiol. **136,** 3884–3891.

Wu, G., Gu, Y., Li, S., and Yang, Z. (2001). A genome-wide analysis of Arabidopsis Rop-interactive CRIB motif–containing proteins that act as Rop GTPase targets. Plant Cell **13,** 2841–2856.

Wu, G., Li, H., and Yang, Z. (2000). Arabidopsis RopGAPs are a novel family of rho GTPase-activating proteins that require the Cdc42/Rac-interactive binding motif for rop-specific GTPase stimulation. Plant Physiol. **124,** 1625–1636.

Wu, L., Bauer, C.S., Zhen, X.G., Xie, C., and Yang, J. (2002). Dual regulation of voltage-gated calcium channels by PtdIns(4,5)P_2. Nature **419,** 947–952.

Wurmser, A.E., Gary, J.D., and Emr, S.D. (1999). Phosphoinositide 3-kinases and their FYVE domain-containing effectors as regulators of vacuolar/lysosomal membrane trafficking pathways. J. Biol. Chem. **274,** 9129–9132.

Yang, W., Burkhart, W., Cavallius, J., Merrick, W.C., and Boss, W.F. (1993). Purification and characterization of a phosphatidylinositol 4-kinase activator in carrot cells. J. Biol. Chem. **268,** 392–398.

Yang, Z. (2002). Small GTPases: Versatile signaling switches in plants. Plant Cell **14** (suppl.), S375–S388.

Zheng, L., Krishnamoorthi, R., Zolkiewski, M., and Wang, X. (2000). Distinct Ca^{2+} binding properties of novel C2 domains of plant phospholipase dalpha and beta. J. Biol. Chem. **275,** 19700–19706.

Zheng, L., Shan, J., Krishnamoorthi, R., and Wang, X. (2002). Activation of plant phospholipase Dbeta by phosphatidylinositol 4,5-bisphosphate: Characterization of binding site and mode of action. Biochemistry **41,** 4546–4553.

Zonia, L., Cordeiro, S., Tupy, J., and Feijo, J.A. (2002). Oscillatory chloride efflux at the pollen tube apex has a role in growth and cell volume regulation and is targeted by inositol 3,4,5,6-tetrakisphosphate. Plant Cell **14,** 2233–2249.

Zonia, L., and Munnik, T. (2004). Osmotically induced cell swelling versus cell shrinking elicits specific changes in phospholipid signals in tobacco pollen tubes. Plant Physiol. **134,** 813–823.